Synthesis and preclinical evaluation of [^{18}F]PF04217903, a selective MET PET tracer

Vegard Torp Lien[1,2], Emily Hauge[1,2], Syed Nuruddin[2], Jo Klaveness[1], Dag Erlend Olberg[1,2].

[1]: Department of Pharmacy, University of Oslo, Oslo, Norway
[2]: Norwegian Medical Cyclotron Center, Oslo, Norway

Abstract

The tyrosine kinase MET (hepatocyte growth factor receptor) is abnormally activated in a wide range of cancers and is often correlated with a poor prognosis. Precision medicine with positron emission tomography (PET) can potentially aid in the assessment of tumor biochemistry and heterogeneity, which can prompt the selection of the most effective therapeutic regimes. The selective MET inhibitor PF04217903 (**1**) formed the basis for a bioisosteric replacement to the deoxyfluorinated analogue [^{18}F]**2**, intended as a PET tracer for MET. [^{18}F]**2** could be synthesized with a "hydrous fluoroethylation" protocol in 6.3 ± 2.6% radiochemical yield and a molar activity of >50 GBq/µmol. *In vitro* autoradiography indicated that [^{18}F]**2** specifically binds to MET in PC3 tumor tissue, and *in vivo* biodistribution in mice showed predominantly a hepatobiliary excretion along with a low retention of radiotracer in other organs.

Introduction

Throughout the past decades, there has been a steady increase in available therapies for cancer treatment. A drug class seeing a surge in new available molecular entities are the protein kinase inhibitors (PKIs).[1] Compared to conventional chemotherapy, these targeted drugs specifically inhibit enzymes that are associated with tumor growth, potentially resulting in better drug response and fewer side effects.[2] However, the response rate is still low, likely due to an inherent population of non-responders, reflecting the heterogeneous nature and individual characteristics of cancers.[3] In cancer therapy, early intervention with the correct drug is paramount for successful treatment. In this respect, positron emission tomography (PET), a non-invasive imaging technique, can be a valuable tool to elucidate the tumor biochemistry and thereby support rapid and suitable treatment.[4]

The tyrosine kinase MET is an important driver in carcinogenesis and metastasis, and its expression correlates with a poor prognosis.[5] For this reason, MET has been extensively studied as a drug target in cancer.[6] Today, the PKIs cabozantinib and crizotinib are regulatory approved, both with nanomolar potency for MET. They are, however, not selective for MET, and a selective radiotracer is preferred for the assessment of MET status *in vivo*. One example of such a selective MET inhibitor is PF04217903 (**1**).[7] Previously, this compound has formed the basis for the development of an optical imaging agent for MET,[8] and may equally well serve as a lead compound for a selective MET PET radiotracer. Due to the bioisosterism of hydroxyl and fluorine,[9] a bioisosteric replacement to the deoxyfluorinated analogue **2** was rationalized (Figure 1). The known structure-activity relationship of **1** suggest that structural modifications at the pyrazole can be performed without significantly affecting the MET affinity.[7] Importantly, both **1** and **2** have lower log P values than kinase inhibitors in general (mean log P 4.2).[10] A more hydrophilic molecule is expected to display a lower degree of protein binding and faster blood clearance, which are desirable attributes for successful tumor imaging with PET.[11]

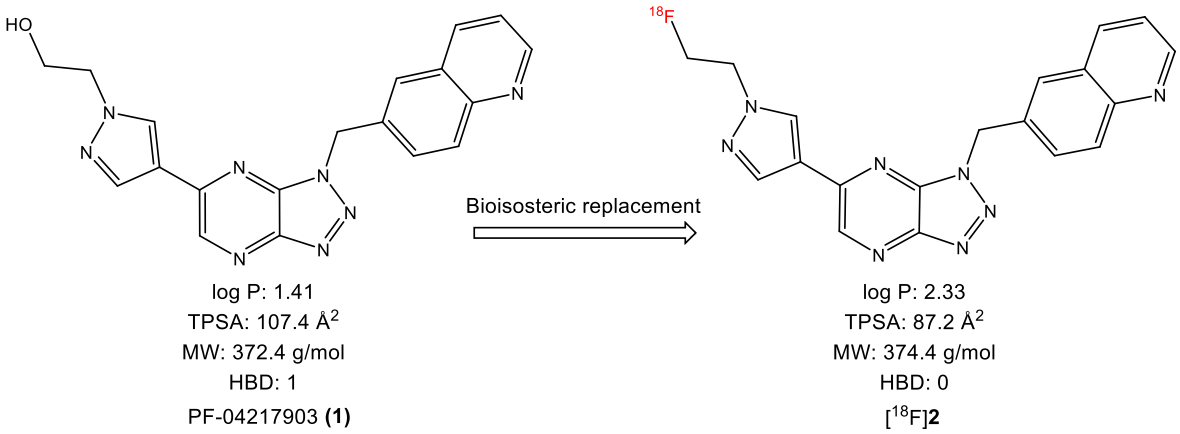

Figure 1: *Bioisosteric replacement of the hydroxyl group in **1** with fluorine, leading to [^{18}F]**2**. Physiochemical properties were predicted with the SwissADME application.*[12]

Several strategies to image MET expression *in vivo* has been explored, predominantly using peptides or monoclonal antibodies.[13] For radiotracers based on small molecular weight compounds targeting the intracellular domain of MET, there is so far only one report.[14] As therapeutic PKIs bind intracellularly, radiotracers binding to the same active site may be important to properly asses target expression and engagement. Herein, the synthesis and preclinical evaluation of [^{18}F]**2** as a PET tracer for the imaging of the MET kinase are presented.

Results and discussion

Chemistry

Starting from **1**, we initially explored a one-step nucleophilic reaction for the synthesis of [^{18}F]**2**. The alcohol **1** was synthesized as previously described,[7] and as illustrated in route A in Scheme 1, the hydroxyl group was intended converted to a good leaving group (**3**), for the subsequent displacement with [^{18}F]fluoride. However, a very low conversion to **3** was observed, even with various strategies, elevated temperatures, excess of reagents and pressurized systems.

Therefore, a modified strategy was rationalized for the synthesis of **3**, and route B in Scheme 1 was investigated. Here, the bromo triazolopyrazine **4**, an intermediate in the synthesis of **1** (Supporting Information, Scheme S1) was exploited. Suzuki coupling of **4** with commercial 1-Boc-pyrazole-4-boronic acid pinacol ester, followed by Boc-deprotection yielded the pyrazole **5**. Further reaction of **5** with ethylene di(*p*-toluenesulfonate) **6** would yield the potential precursor **3**. Unexpectedly, only the hydroxyl compound **1** was observed as a product in this reaction. Here, hydrolysis of the tosyl group must occur, pointing towards a stabilizing effect of the hydroxyl group in **1**. An intramolecular hydrogen bond between the pyrazole nitrogen and hydroxyl group can explain the outcomes of both routes A and B (Supporting Information, Figure S1). A third strategy was then devised, this time a two-step radiochemical reaction with 2-[^{18}F]fluoroethyl tosylate ([^{18}F]FETos) (Route C, Scheme 1). With pyrazole **5** already in hand, cold reference compound **2** could be synthesized with fluoroethyl tosylate, suggesting that this approach could be a viable synthetic route using [^{18}F]FETos.

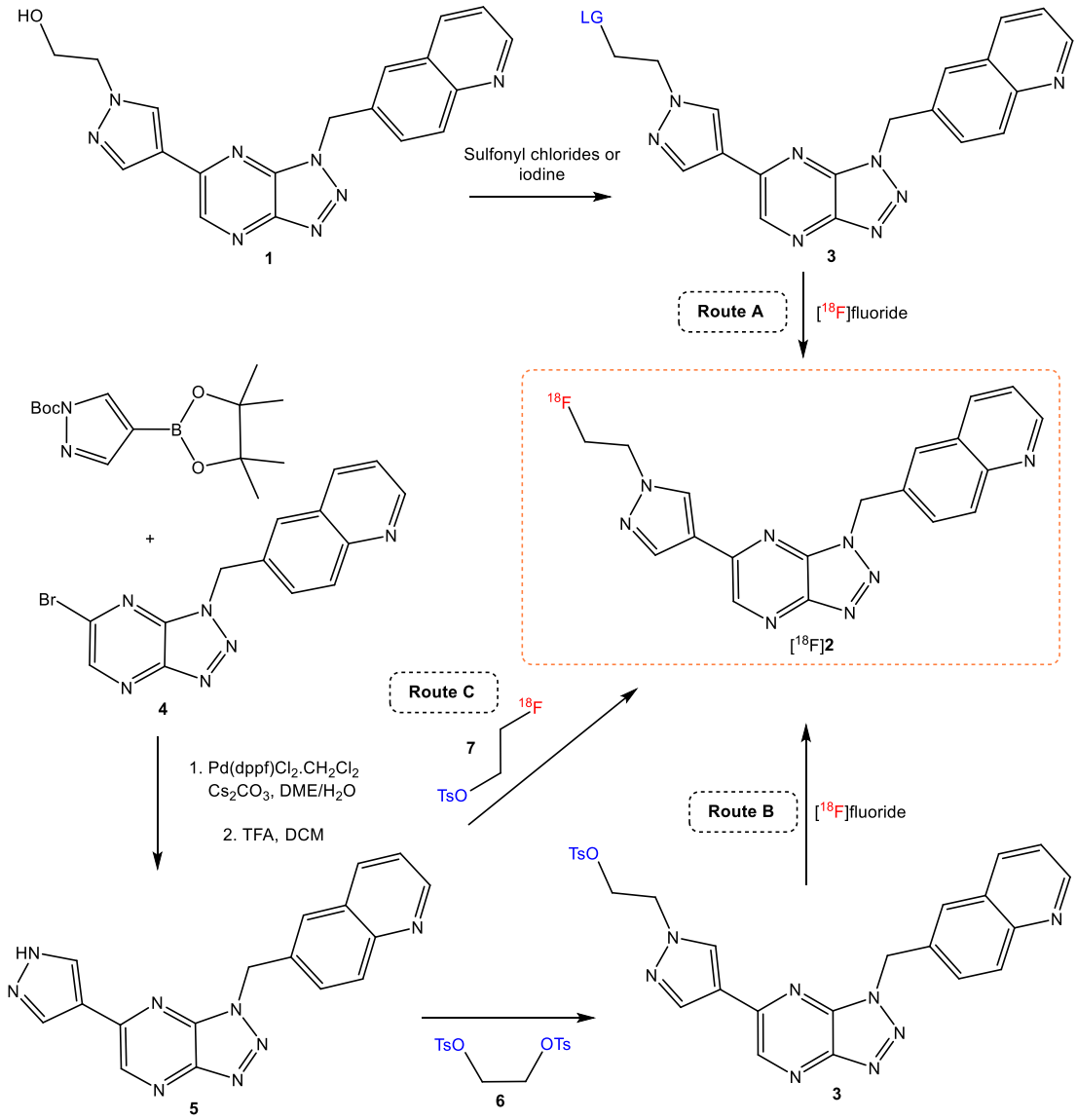

Scheme 1: *Synthetic routes explored towards a possible precursor and [^{18}F]**2**. Route A and B failed, while radiolabelled and non-radiolabelled **2** could be obtained with route C.*

[^{18}F]FETos is a versatile prosthetic group in PET radiochemistry,[15] and would provide [^{18}F]**2** from the nucleophilic attack of **5**. [^{18}F]FETos is normally purified before further reactions, although there are reports where intermediate purification is omitted. Initial experiments with a conventional method as earlier reported[16] gave only low yields of both [^{18}F]FETos and [^{18}F]**2**. Appealing by its simplistic approach, we explored the "hydrous fluoroethylation" conditions reported by Kneiss et al.[17] This protocol avoids the azeotropic drying by eluting the trapped [^{18}F]fluoride with a 2% solution of water in acetonitrile (with K_2CO_3 and K222) directly to a reaction vial containing **6** and Cs_2CO_3 (Scheme 2). Produced [^{18}F]FETos was then reacted directly with **5** to yield [^{18}F]**2** without intermediate purification. This approach reduced synthesis time as compared to the conventional method and was less burdensome to automate.

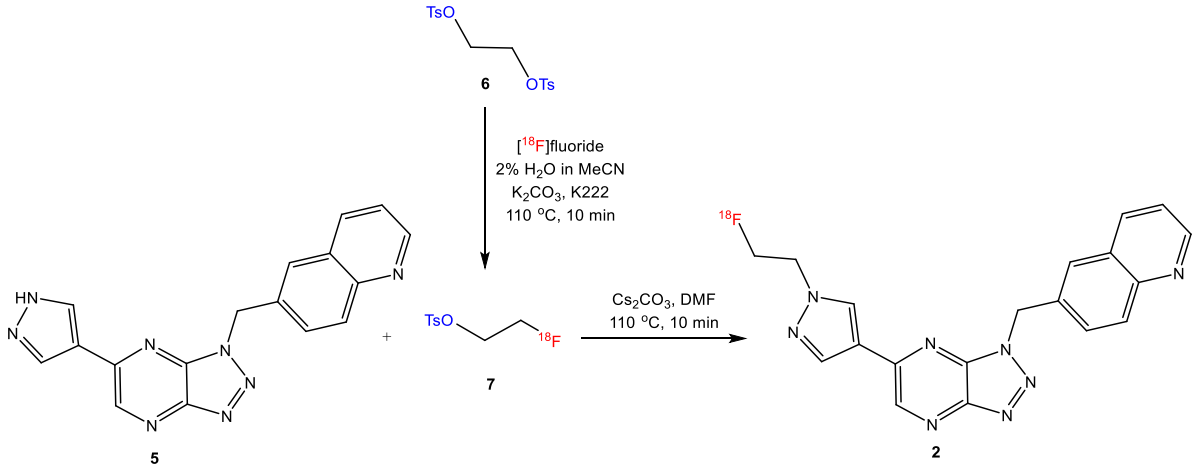

Scheme 2: *Two-step synthesis of [^{18}F]**2** with a "hydrous fluoroethylation" protocol.*

With the conditions in Scheme 2, [^{18}F]FETos could be achieved in good yields (85%, n = 3). Further on, close to full conversion of [^{18}F]FETos into [^{18}F]**2** (Table 1, entry 1) was achieved with Cs_2CO_3 in DMF. Despite these promising initial results, different solvents and bases were explored for the incorporation of [^{18}F]FETos. Specifically, a soluble base and a solvent with lower elution strength were sought to avoid potential solubility problems during automation and poor chromatography, respectively.

Table 1: *Optimization of reaction conditions for the incorporation of [^{18}F]FETos to yield [^{18}F]**2**.*

Entry	Solvent	Base	Conversion[a,b]
1	DMF	Cs_2CO_3	99% (n = 2)
2	DMF	-	40% (n = 1)
3	MeCN	-	45% (n = 2)[c]
4	MeCN	Cs_2CO_3	51% (n = 1)[c]
5	DMF	Et_3N	11% (n = 2)
6	THF	Cs_2CO_3	83% (n = 2)

[a]: Reaction conditions: Produced [^{18}F]FETos was aliquoted into reaction vials, and precursor **5** (4.5 mg, 0.014 mmol) and base (0.014 mmol) in appropriate solvent (300 µL) were added. The reaction mixture was heated to 110 °C for 10 min.
[b]: Conversion calculated as percent incorporation of [^{18}F]FETos into [^{18}F]**2**. Average is given when applicable.
[c:] Precursor **5** was poorly dissolved in MeCN.

Since Cs_2CO_3 is present in the synthesis of [^{18}F]FETos, we investigated if base in the second step could be omitted. However, this led to a considerably reduced conversion (Table 1, entry 2). Both MeCN instead of DMF, and NEt_3 instead of Cs_2CO_3 gave reduced conversion to [^{18}F]**2** (Table 1, entries 3-5). Cs_2CO_3 in THF gave an acceptable conversion (Table 1, entry 6), but THF was deemed unsuitable due to its low boiling point and pressure build-up in the reaction vessel. Further on, the reaction time profile was analysed by HPLC at 5, 10 and 20 minutes, with no increase in yield after 10 minutes. Based on the above findings, DMF, Cs_2CO_3 and 10 minutes reaction time were implemented in the automation of the radiochemistry. Here, [^{18}F]**2** was obtained in 6.3 ± 2.6% radiochemical yield (n = 5) after semi-preparative HPLC purification. Chemical and radiochemical purity was > 95%, with a molar activity of > 50 GBq/µmol. Radio-TLC confirmed the radiochemical purity. It can be noted that when higher

amounts of radioactivity was used (> 10 GBq), a significant portion (up to 80%) of the [^{18}F]fluoride remained on the anion exchange column, indicating that a 2% solution of water is borderline of what is needed for the proper release of [^{18}F]fluoride. However, this could be mitigated by reducing the amount of resin material (from 130 to 30 mg). Overall, this "hydrous fluoroethylation" protocol afforded compound [^{18}F]**2** in better yield and was in our hands easier to implement than the conventional production method of [^{18}F]FETos.

Biology

Enzymatic assay

To evaluate whether the bioisosteric replacement had impacted the MET affinity, **2** was evaluated in an enzymatic MET assay. Here it was seen that the fluorine analogue **2** performed better than the parent compound **1**, with IC_{50} values of 176 and 612 nM, respectively. As an additional assay reference, cabozantinib was evaluated with an IC_{50} value of 86 nM (Supporting Information, Figure S12).

Kinase selectivity

A preferable characteristic of **2** is the selectivity for MET over other kinases, and a kinase selectivity screen was performed on a selection of kinases (Table 2). This selection was based on the binding pattern of other PKIs with known affinity for MET. In this assay, compound **2** displayed a similar selectivity for MET as the parent compound **1**, suggesting that the fluorine for hydroxyl replacement is well tolerated and preserved the MET selectivity.

Table 2: Kinase selectivity for PF04217903 and **2**.

Compound	% inhibition at 1 µM						
	RET	**ALK**	**ROS**	**MET**	**VEGFR2**	**EGFR (WT)**	**KIT**
PF04217903 (**1**)	5	8	3	99	6	8	0
2	5	5	4	97	7	5	6

In vitro autoradiography

In vitro autoradiography was performed with sections from PC3 tumor tissue, a prostate cancer cell line known to have high expression of MET.[18,19] A robust binding of [^{18}F]**2** to tumor tissue was observed, with a reduction in total binding when co-incubated with either **1** or cabozantinib (Figure 2). Due to the large structural similarities between [^{18}F]**2** and **1**, cabozantinib was included as a blocker to ensure that both non-specific and off-target binding was evaluated. In summary, these results indicate that [^{18}F]**2** is specifically binding to MET *in vitro*.

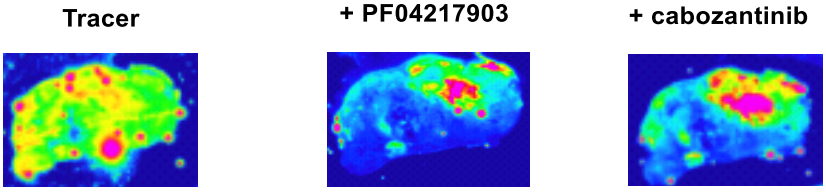

***Figure 2**: In vitro autoradiography on PC3 tumor sections, incubated with [^{18}F]**2**, [^{18}F]**2** + PF04217903 or [^{18}F]**2** + cabozantinib.*

Metabolic stability

The *in vivo* metabolic stability of [^{18}F]**2** was evaluated at 5, 20 and 60 minutes with TLC analysis. After 20 minutes, 58% intact tracer was present, while mostly polar metabolites were present after 60 minutes (< 10% intact tracer). The metabolites were retained on the origin of the TLC plate, making it difficult to discriminate between free [^{18}F]fluoride and other polar metabolites. However, PET imaging experiments in mice revealed little bone accumulation over 90 min, indicating that *in vivo* defluorination is negligible.

Biodistribution

In vivo assessment of [^{18}F]**2** was performed in naive mice with a dynamic µPET scan over 90 minutes, along with *ex vivo* biodistribution at 10 and 60 minutes post injection (Figure 3).

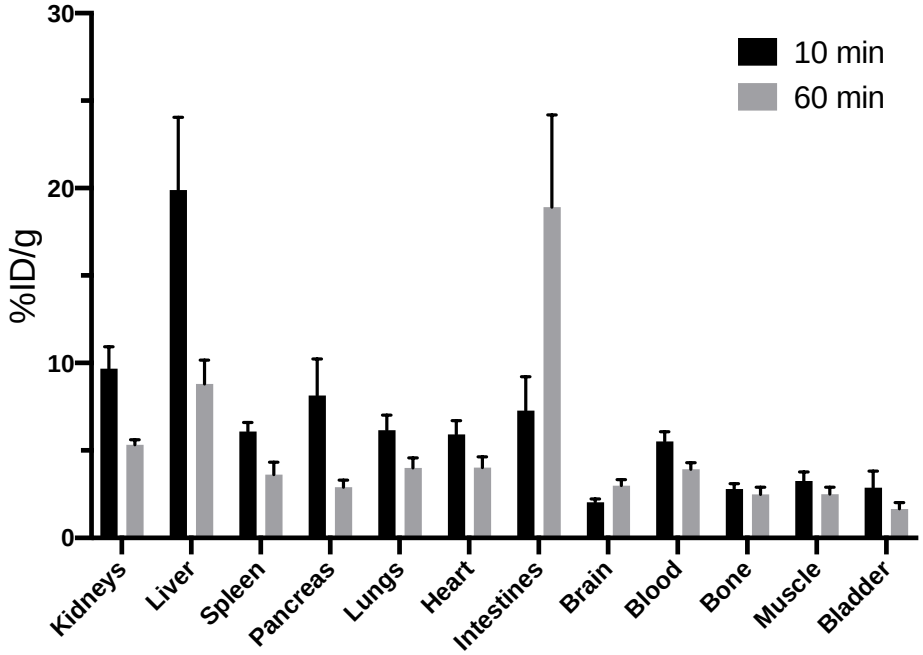

Figure 3: *Ex vivo* biodistribution of [^{18}F]**2** in naive mice at 10 and 60 minutes post injection, given in % ID/g.

Rapid accumulation of activity in the liver (19.9 ± 4.1% ID/g) was observed with *ex vivo* biodistribution, indicating a hepatobiliary metabolic route. Predominant liver uptake was also observed with µPET. At 60 minutes, the main portion of the activity was found in the intestines (18.9 ± 5.3% ID/g), with reduction in uptake elsewhere. Activity in blood and muscle were declining during the evaluated time period, indicating a washout from background tissue.

Conclusion

Rationalized from a bioisosteric replacement, [^{18}F]**2** could be synthesized with a two-step fluoroethylation protocol without azeotropic drying or intermediate purification. [^{18}F]**2** was obtained in 6.3 ± 2.6% radiochemical yield with > 95% chemical and radiochemical purity and > 50 GBq/µmol molar activity. *In vitro*, **2** displayed similar high kinase selectivity as parent **1**. *In vitro* autoradiography indicated selective binding to MET in PC3 tumor tissue, while i*n vivo* evaluation in naive mice showed a relatively rapid metabolism, with 58% of the tracer remaining intact after 20 minutes. *Ex vivo* biodistribution indicated little or no bone uptake, and favourable washout from blood and muscle. Overall, [^{18}F]**2** could serve as a valuable tool for the quantification of MET *in vivo*.

Experimental

Chemistry

General

All chemicals were purchased from Sigma–Aldrich or Fluorochem and used without further purification unless otherwise noted. Air and/or moisture sensitive reactions were performed under argon atmosphere with dried solvents and reagents. TLC was performed on Merck silica gel 60 F_{254} plates and visualized with UV light at 312 nm or 365 nm. Column chromatography was performed with silica gel (pore size 60 Å, 230–400 mesh particle size) purchased from Fluka. ^{1}H and ^{13}C NMR spectra were obtained on a Bruker AVIII HD 400 instrument (400/101 MHz). ^{19}F NMR spectra were obtained on a Bruker DPX 200 instrument (188 MHz). Chemical shifts (δ) are reported in parts per million, and coupling constants are reported in Hertz (Hz). The residual proton solvent resonance in ^{1}H NMR ($CDCl_3$ at δ 7.27, DMSO-d_6 at δ 2.50) and the residual carbon solvent resonance in ^{13}C NMR ($CDCl_3$ at δ 77.16 ppm and DMSO-d_6 at δ 39.52) are used as reference. Accurate mass determination (HRMS) was performed on a Waters Prospec Q instrument, ionized by electrospray (ESI). LC-PDA-MS was performed on a Thermo Finnigan LCQ Deca XP Plus, equipped with a Kinetex 2.6 µm EVO 100 Å column (50x2.1 mm, 500 µL/min), with a gradient from 10 to 90% MeCN in water containing 0.05% TFA.

6-((6-(1H-Pyrazol-4-yl)-1H-[1,2,3]triazolo[4,5-b]pyrazin-1-yl)-methyl)quinoline (**5**)

6-((6-Bromo-1H-[1,2,3]triazolo[4,5-b]pyrazin-1-yl)-methyl)quinoline (**4**) (100 mg, 0.29 mmol, intermediate in the synthesis of **2**, see Supporting Information), 1-Boc-4-(4,4,5,5-tetramethyl-1,3,2-dioxaborolan-2-yl)pyrazole (88 mg, 0.30 mmol) and Cs_2CO_3 (330 mg, 1.01 mmol) were added to a sealed tube under an argon atmosphere. DME (4 mL) and H_2O (1 mL) were added, and the reaction mixture was degassed for 15 minutes, before $Pd(dppf)Cl_2 \cdot CH_2Cl_2$ (18 mg, 0.022 mmol) was added. The solution was degassed again for 5 minutes and stirred for 24 hours at 80 °C. EtOAc (5 mL) and water (5 mL) were added and the phases separated. The aqueous phase was extracted with EtOAc (3x5 mL) and the combined organic fractions were washed with water (5 mL) and brine (5 mL), dried over $MgSO_4$ and concentrated under reduced pressure. The dried product was redissolved in DCM (10 mL), added TFA (1 mL) and stirred at ambient temperature for 2 hours. Water (15 mL) was added, phases separated, and the organic phase was extracted with water (2x10 mL). The collected aqueous fractions were basicified to pH 12 with NaOH (1M). A solid crashed out and filtration provided the title compound as a grey solid (94 mg, 98% yield). ^{1}H NMR (400 MHz, DMSO-d_6): δ 13.44 (s, 1H), 9.25 (s, 1H), 8.89 (dd, J = 4.2, 1.7 Hz, 1H), 8.71 (s, 1H), 8.38 (dd, J = 8.3, 1.3 Hz, 1H), 8.32 (s, 1H), 8.05-7.99 (m, 2H), 7.83 (dd, J = 8.8, 2.0 Hz, 1H), 7.52 (dd, J = 8.3, 4.2 Hz, 1H), 6.15 (s, 2H). ^{13}C NMR (101 MHz, DMSO-d_6): δ 150.36, 148.07, 146.63, 146.24, 141.61, 137.82, 137.12, 135.49, 132.85, 128.96, 128.90, 127.05, 126.74, 121.28, 118.18, 49.43. HRMS (ESI+) *m/z* calcd. for $C_{17}H_{12}N_8Na$ $[M+ Na]^+$: 351.1007, found 351.1007).

6-((6-(1-(2-Fluoroethyl)-1H-pyrazol-4-yl)-1H-[1,2,3]triazolo[4,5-b]pyrazine-1-yl)methyl)quinolone (**2**)

6-((6-(1H-Pyrazol-4-yl)-1H-[1,2,3]triazolo[4,5-b]pyrazin-1-yl)-methyl)quinoline (**5**) (40 mg, 0.122 mmol) and Cs_2CO_3 (88 mg, 0.27 mmol) were dissolved in DMF (2 mL), and added 2-fluoroethyl-4-methylbenzenesulfonate (**7**) (44 µL, 0.24 mmol). The reaction mixture was stirred at 80 °C for 15 hours. DCM (5 mL) and water (5 mL) were added and phases separated. The aqueous phase was extracted with DCM (3x5 mL) and the collected organic fractions were washed with water (5 mL) and brine (5 mL), dried over $MgSO_4$ and concentrated under reduced pressure. The crude product was purified with

column chromatography (DCM:MeOH, 100:2) and the title compound was obtained as a white solid (15 mg, 33% yield). ^{1}H NMR (400 MHz, DMSO-d_6): δ 9.22 (s, 1H), 8.89 (dd, *J* = 4.2, 1.7 Hz, 1H), 8.71 (s, 1H), 8.42–8.35 (m, 2H), 8.07 – 8.00 (m, 2H), 7.84 (dd, *J* = 8.7, 2.1 Hz, 1H), 7.55 (dd, *J* = 8.3, 4.2 Hz, 1H), 6.16 (s, 2H), 4.89 (t, *J* = 4.7 Hz, 1H), 4.78 (t, *J* = 4.7 Hz, 1H), 4.59 (t, *J* = 4.7 Hz, 1H), 4.52 (t, *J* = 4.7 Hz, 1H). ^{13}C NMR (101 MHz, DMSO): δ 150.65, 147.76, 146.74, 146.53, 141.60, 138.57, 137.34, 135.86, 133.09, 131.27, 129.14, 129.11, 127.30, 126.96, 121.61, 119.11, 81.4 (d, *J* = 168.3 Hz), 51.9 (d, *J* = 19.5 Hz), 49.69. ^{19}F NMR (188 MHz, DMSO-d_6): δ -222.1. HRMS (ESI+) *m/z* calc. $C_{19}H_{15}FN_8Na$ $[M+ Na]^+$: 397.1296, found 397.1296.

2-Fluoroethyl-4-methylbenzenesulfonate (**7**)
p-Toluensulfonyl chloride (3.69 g, 19.4 mmol), fluoroethanol (1.0 g, 15.6 mmol) and DMAP (3.94 g, 32.6 mmol) were dissolved in DCM (50 mL) under an argon atmosphere. Triethylamine (2.60 mL, 18.7 mmol) was added to the reaction mixture at 0 °C, and the reaction mixture was stirred at ambient temperature overnight. DCM (50 mL) and water (50 mL) were added, and the phases were separated. The aqueous phase was extracted with DCM (3x30 mL), and the collected organic fractions were washed with $NaHCO_3$ (20 mL) and HCl (20 mL), dried over $MgSO_4$ and concentrated under reduced pressure to provide the title compound as a brown oil (0.67 g, 20% yield). The spectroscopic analysis was in agreement with earlier reported data.[20] ^{1}H NMR (400 MHz, $CDCl_3$): δ 7.79 (d, *J* = 8.3 Hz, 2H), 7.35 (d, *J* = 8.1 Hz, 3H), 4.62 (t, *J* = 4.1 Hz, 1H), 4.50 (t, *J* = 4.1 Hz, 1H), 4.28 (t, *J* = 4.1 Hz, 1H), 4.21 (t, *J* = 4.1 Hz, 1H), 2.44 (s, 3H).

Radiochemistry

General
[^{18}F]Fluoride was produced from the ^{18}O(p,n)^{18}F nuclear reaction on a GE PETtrace 880 cyclotron. Radiosyntheses and azeotropic drying were performed on a ScanSys chemistry module (Værløse, Denmark). HPLC analyses were performed on an Agilent system (1100 series) with UV- and radiodetector equipped with a ACE 3 µm C18-AR 50×4.6mm column (10 to 90% acetonitrile in water (0.05% TFA) over 10 minutes, flow 1mL/min). Radio-TLC was analysed with a Raytest MiniGita (Straubenhardt, Germany). The eluent solution for the release of [^{18}F]fluoride from QMA column after cyclotron production was prepared as follows: K_2CO_3 (207 mg, 1.5 mmol) was dissolved in 1 mL water to make a 1.5 M solution. 100 µL of this solution was added to K_{222} (113 mg, 3 mmol) dissolved in 5 mL MeCN. Ethylene di(*p*-toluenesulfonate) was recrystallized from EtOH before use.

Manual radiosynthesis of 6-((6-(1-(2-[^{18}F]fluoroethyl)-1H-pyrazol-4-yl)-1H-[1,2,3]triazolo[4,5-b]pyrazine-1-yl)methyl)quinolone ([^{18}F]**2**)
[^{18}F]Fluoride was separated from ^{18}O enriched water with a Sep-Pak QMA Light cartridge (130 mg, activated with H_2O (5 mL) and air (5 mL)). After loading, the cartridge was rinsed with 1.5 mL MeCN. [^{18}F]fluoride was released with the solution described above into a vial with ethylene di(*p*-toluenesulfonate) (**6**) (7.2 mg, 0.019 mmol) and Cs_2CO_3 (6.6 mg, 0.020 mmol). The reaction mixture was heated to 100 °C for 15 min, and HPLC analysis was performed to confirm product identity, with **7** as an internal standard. The yield of [^{18}F]FETos was determined from the incorporation of [^{18}F]fluoride. Produced [^{18}F]FETos was aliquoted to new reaction vials, and precursor **5** (4.6 mg, 0.014 mmol) and base dissolved in a solvent (300 µL) were added. The mixture was heated at 110 °C for 10 minutes, and analysed by HPLC. The yield of [^{18}F]**2** was determined from the incorporation of [^{18}F]FETos**.**

*Automated radiosynthesis of [^{18}F]**2**.*

[^{18}F]Fluoride were transferred from the cyclotron to the hotcell, and separated from ^{18}O enriched water with a Sep-Pak QMA Light cartridge (30 mg, activated with H_2O (5 mL) and air (5 mL)). [^{18}F]Fluoride was released with the solution described above into a vial with ethylene di(*p*-toluenesulfonate) (**6**) (7.2 mg, 0.019 mmol) and Cs_2CO_3 (6.6 mg, 0.020 mmol). The reaction mixture was heated to 100 °C for 15 min. Precursor **5** (4.5 mg, 0.014 mmol) and Cs_2CO_3 (4.6 mg, 0.014 mmol) dissolved in DMF (300 µL) were added manually (tongs) with a syringe and the reaction mixture was heated for 10 min at 110 °C. The crude reaction mixture was dissolved in 2 mL of 12% MeCN in water, and semi-preparative HPLC was used for purification (12% MeCN in water, 0.5% TFA). The collected product was diluted with water (10 mL) and retained on a Sep-Pak tC18 Plus Light cartridge (activated with EtOH (5 mL) and water (5 mL)). The final product was released with EtOH (0.5 mL). HPLC analysis was performed to evaluate the purity and identity of the product.

Biological evaluation

Animal handling

Athymic nude mice (Athymic Nude-Foxn1^{nu}; weight, 34-40 g; age, 12-13 weeks) were used. The protocol was approved by The National Animal Research Authority, and the experiment was conducted according to the regulations of the Federation of European Laboratory Animal Science Association (FELASA). All animals were kept in a standard animal housing environment at the institutional Department of Comparative Medicine, University of Oslo, and kept under pathogen-free conditions, at constant temperature (21.5 ± 0.5 °C) and humidity (55 ± 5%), 20 air changes/h and a 12 h light/dark cycle. Distilled tap water was given ad libitum. Following overnight fasting, the animals were anesthetized and a catheter flushed with heparinized saline was inserted in the tail vein.

MicroPET scan

A 50 min PET acquisition in list mode was started prior to i.v. administration of 5-10 MBq [^{18}F]**2** (diluted in heparinized saline) under anesthesia and mice were anesthetized with 2% isoflurane in 2 L/min oxygen. Anesthesia was maintained by inhalation of approximately 1.5% isoflurane/O_2 at 1 l/min. Attenuation and scatter correction was obtained by acquiring a 10 min transmission scan with a ^{68}Ge point source. The 3D dynamic emission data were reconstructed using OSEM-MAP (2 OSEM iterations, 18 MAP iterations, $\beta = 0.5$, matrix size $= 128 \times 128 \times 95$), producing images with voxel size $0.87 \times 0.87 \times 0.80$ mm^3. The sampling time ranged from 15 s (early time points) to 600 s (late time points). All images were saved in the DICOM format and transferred to a remote PC for post-processing and kinetic modeling using in-house-written IDL programs (Interactive Data Langue, v 6.2, Research Systems Inc., Boulder, CO).

In vivo biodistribution

After injection of [^{18}F]**2** (1.2-1.8 MBq), the mice were decapitated after 10 (n = 4) and 60 (n = 3) minutes. Organs were collected in preweighed tubes, and activity was counted with a well counter (Packard BioScience Company Cobra II Auto-Gamma Counter Model D5005, USA). All collected data were decay corrected to the injected dose, and tissue distributions are given as % ID/g.

Metabolic stability

After injection of 8-10 MBq of [^{18}F]**2**, the mice were decapitated at 5, 20 and 60 minutes (n = 1 for each time point), and blood was collected in EDTA tubes. The blood was spun for 5 minutes at 4000 rpm. The supernatant was placed in a second vial, and equal volume of MeCN was added before centrifugation for 5 minutes at 4000 rpm. The resulting plasma supernatant was analysed on TLC plates,

eluted with MeCN. The plates were placed in a cassette with a phosphor storage screen (Fujifilm SR High Res), and the film was exposed overnight, and read with a Fujifilm BAS-5000 plate reader. Percent remaining parent tracer could then be calculated.

In vitro autoradiography
PC3 tumour sections (20 µm) were thawed for 15 min, dried and preincubated in buffer for 10 min at room temperature. After drying, the sections were incubated at room temperature for 30 min with 200 µL of a solution of [^{18}F]**2** in buffer containing either 10 µM of a blocking agent (PF04217903 or cabozantinib) or 10 µM DMSO (n = 3 for each condition). After incubation, the sections were washed 2x5 min in cold buffer with BSA (0.1-0.3%). After a quick dip in cold water, the sections were dried and placed in a cassette with a phosphor storage screen (Fujifilm SR High Res). The film was exposed overnight, and read with a Fujifilm BAS-5000 plate reader.

MET kinase assay
The enzymatic MET assay was purchased from Cyclex and used following the manufacturer's instructions. Briefly, while placed on ice, recombinant MET was added to wells precoated with substrate, and the reaction was started by adding buffer containing the inhibitors in appropriate dilutions. The plate was incubated at 30 ºC for 60 min. After washing with buffer, a HRP conjugated detection antibody PY-39 was added to each well and incubated at ambient temperature for 60 min. The TMB substrate was added after another round of washing and incubated at ambient temperature for 10 min. Stop solution was added, and absorbance was measured with a spectrophotometric plate reader (Perkin Elmer VICTOR™ X3). The results were analysed with GraphPad Prism, and the assay was carried out in triplicates for each inhibitor.

Acknowledgements

Solveig Pettersen and Mads Haugland Haugen (Department of Tumor Biology, Radiumhospitalet, Oslo) are acknowledged for the MET enzymatic assay. Head engineer Hong Qu (Institute of Basic Medical Sciences, University of Oslo) is acknowledged for assistance with animal experiments. Department of Pharmacy (University of Oslo) is acknowledged for economic support.

References

1. Wu P, Nielsen TE, Clausen MH. FDA-approved small-molecule kinase inhibitors. *Trends Pharmacol Sci*. **2015**;36:422-439.

2. Roskoski R. A historical overview of protein kinases and their targeted small molecule inhibitors. *Pharmacol Res*. **2015**;100:1-23.

3. Huang M, Shen A, Ding J, Geng M. Molecularly targeted cancer therapy : some lessons from the past decade. *Trends Pharmacol Sci*. **2014**;35(1):41-50.

4. Alam IS, Arshad MA, Nguyen QD, Aboagye EO. Radiopharmaceuticals as probes to characterize tumour tissue. *Eur J Nucl Med Mol Imaging*. **2015**;42(4):537-561.

5. Gherardi E, Birchmeier W, Birchmeier C, Vande Woude G. Targeting MET in cancer: rationale and progress. *Nat Rev Cancer*. **2012**;12(2):89-103.

6. Cui JJ. Targeting Receptor Tyrosine Kinase MET in Cancer : Small Molecule Inhibitors and Clinical Progress. *J Med Chem*. **2014**;57:4427-4453.

7. Cui JJ, Mctigue M, Nambu M, et al. Discovery of a novel class of exquisitely selective

mesenchymal-epithelial transition factor (c-MET) protein kinase inhibitors and identification of the clinical candidate 2-(4-(1-(quinolin-6-ylmethyl)-1H-[1,2,3]triazolo[4,5-b]pyrazin-6-yl)-1H-pyrazol-1-y. *J Med Chem*. **2012**;55:8091-8109.

8. Kim E, Yang KS, Weissleder R. Bioorthogonal small molecule imaging agents allow single-cell imaging of MET. *PLoS One*. **2013**;8(11):1-14.

9. Patani GA, Lavoie EJ. Bioisosterism : A Rational Approach in Drug Design. *Chem Rev*. **1996**;96:3147-3176.

10. Heffron TP. Small Molecule Kinase Inhibitors for the Treatment of Brain Cancer. *J Med Chem*. **2016**;59(22):10030-10066.

11. Gee AD, Bongarzone S, Wilson AA. Small Molecules as Radiopharmaceutical Vectors. In: J. S. Lewis et al. (eds.), ed. *Radiopharmaceutical Chemistry*. Springer Nature; 2019.

12. Daina A, Michielin O, Zoete V. SwissADME: a free web tool to evaluate pharmacokinetics, drug-likeness and medicinal chemistry friendliness of small molecules. *Sci Rep*. **2017**;7:42717.

13. Han Z, Wu Y, Wang K, et al. Analysis of progress and challenges for various patterns of c-MET-targeted molecular imaging: a systematic review. *EJNMMI Res*. **2017**;7.

14. Wu C, Tang Z, Fan W, et al. In vivo Positron Emission Tomography (PET) imaging of Mesenchymal - Epithelial Transition (MET) receptor. *J Med Chem*. **2010**;53(1):139-146.

15. Kniess T, Laube M, Brust P, Steinbach J. 2-[^{18}F]Fluoroethyl tosylate - a versatile tool for building ^{18}F-based radiotracers for positron emission tomography. *Med Chem Commun*. **2015**;6(10):1714-1754.

16. Veach DR, Namavari M, Pillarsetty N, et al. Synthesis and Biological Evaluation of a Fluorine-18 Derivative of Dasatinib. *J Med Chem*. **2007**;50:5853-5857.

17. Kniess T, Laube M, Steinbach J. "Hydrous ^{18}F-fluoroethylation"– Leaving off the azeotropic drying. *Appl Radiat Isot*. **2017**;127(June):260-268.

18. Knudsen BS, Edlund M. Prostate cancer and the Met hepatocyte growth factor receptor. *Adv Cancer Res*. **2004**;91:31-67.

19. Yin B, Liu Z, Wang Y, et al. RON and c-Met facilitate metastasis through the ERK signaling pathway in prostate cancer cells. *Oncol Rep*. **2017**;37(6):3209-3218.

20. Moussa IA, Banister SD, Beinat C, Giboureau N, Reynolds AJ, Kassiou M. Design, Synthesis, and Structure−Affinity Relationships of Regioisomeric N-Benzyl Alkyl Ether Piperazine Derivatives as σ-1 Receptor Ligands. *J Med Chem*. **2010**;53(16):6228-6239.